Scavenger receptor MARCO is associated with an immunosuppressive microenvironment and tumour progression in intrahepatic CCA

Aloña Agirre-Lizaso,[1] Maider Huici-Izagirre,[1] Colm J O'Rourke,[2] Ekaterina Zhuravleva,[2] Ana Korosec,[3] Mikel Azkargorta,[4,5] Felix Elortza,[4,5] Javier Vaquero,[6] Sumera I Ilyas,[7] Gregory J Gores,[7] Jesper B Andersen,[2] Gernot Schabbauer,[3] Luis Bujanda,[1,4] Pedro M. Rodrigues,[1,4,8] Omar Sharif,[3] Jesus M. Banales,[1,4,8,9] Maria J. Perugorria.[1,4,10]

[1] Department of Liver and Gastrointestinal Diseases, Biodonostia Health Research Institute - Donostia University Hospital -, University of the Basque Country (UPV/EHU), San Sebastian, Spain; [2] Biotech Research and Innovation Centre (BRIC), Department of Health and Medical Sciences, University of Copenhagen, Copenhagen, Denmark; [3] Institute for Vascular Biology, Centre for Physiology and Pharmacology, Medical University Vienna, Vienna, Austria; Christian Doppler Laboratory for Arginine Metabolism in Rheumatoid Arthritis and Multiple Sclerosis, Vienna, Austria; [4] CIBERehd, Instituto de Salud Carlos III (ISCIII), Madrid, Spain; [5] Proteomics Platform, CIC bioGUNE, ProteoRed-ISCIII, Bizkaia Science and Technology Park, Derio, Spain; [6] TGF-β and Cancer Group, Oncobell Program, Bellvitge Biomedical Research Institute (IDIBELL), Barcelona, Spain; National Biomedical Research Institute on Liver and Gastrointestinal Diseases (CIBERehd), Instituto de Salud Carlos III, Madrid, Spain; Sorbonne Université, Inserm, Centre de Recherche Saint-Antoine (CRSA), Paris, France; [7] Division of Gastroenterology and Hepatology, Mayo Clinic, Rochester, Minnesota; [8] IKERBASQUE, Basque Foundation for Science, Bilbao, Spain; [9] Department of Biochemistry and Genetics, School of Sciences, University of Navarra, Pamplona, Spain; [10] Department of Medicine, Faculty of Medicine and Nursing, University of the Basque Country (UPV/EHU), Leioa, Spain.

BACKGROUND

- **Cholangiocarcinoma (CCA)** comprises a heterogeneous group of malignant tumors with dismal prognosis.
- In CCA, **immune cells** present in the tumour microenvironment have been reported to support tumour progression.
- Targeting the immune system in CCA is a promising approach for **anti-cancer therapy.**
- **Scavenger receptor MARCO** plays a determining tole in macrophage polarization and consequently in adaptive immune responses in many solid tumours.

AIMS

Understand the role of scavenger receptor MARCO in intrahepatic CCA (iCCA) development and progression.

Evaluate the potential role of MARCO as a novel prognostic and therapeutic target.

METHODS

- Evaluation of cell-type specific *MARCO* expression in iCCA human tumours in **single-cell RNA sequencing** data from different studies and functional characterization of *MARCO*-expressing TAMs.
- Analysis of ***MARCO* mRNA expression** in liver tissue samples from patients with iCCA compared to control individuals and correlation with clinicopathological parameters.
- Association of *MARCO* expression to the immunological microenviroment in iCCA employing **bioinformatic tools**.
- Study of the role of *Marco* in the development and progression of **iCCA mouse models**.
- **Flow cytometry** analysis of the TME in iCCA models of WT and *Marco*$^{-/-}$ mice.

CONTACT

matxus.perugorria@biodonostia.org

jesus.banales@biodonostia.org

RESULTS

Figure 1: *MARCO* expression in human iCCA liver samples

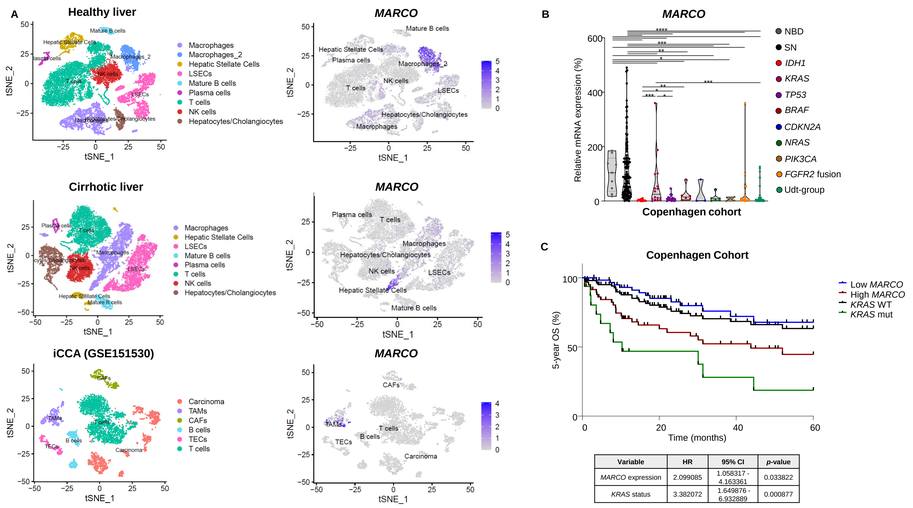

Variable	HR	95% CI	*p*-value
MARCO expression	2.099085	1.058317 - 4.163361	0.033822
KRAS status	3.382072	1.649876 - 6.932889	0.000877

(**A**) Analysis of cell-type-specific *MARCO* expression in normal, cirrhotic and iCCA livers by single-cell RNA sequencing; (**B**) *MARCO* mRNA (microarray) expression in normal bile duct (n=9) and surrounding normal human tissue (n=143) compared to *IDH1* (n=16), *KRAS* (n=16), *TP53* (n=17), *BRAF* (n=6), *CDKN2A* (n=3), *NRAS* (n=6), *PIK3CA* (n=4), *FGFR2* mutant (n=18) iCCA tumors or harboring no mutations in any of those genes, Udt-group (n=64); (**C**) Multivariate analysis of 5-year overall survival of patients with iCCA according to *MARCO* expression levels and *KRAS* driving mutation status.

Figure 2: Functional characterization of *MARCO*-expressing TAMs in iCCA

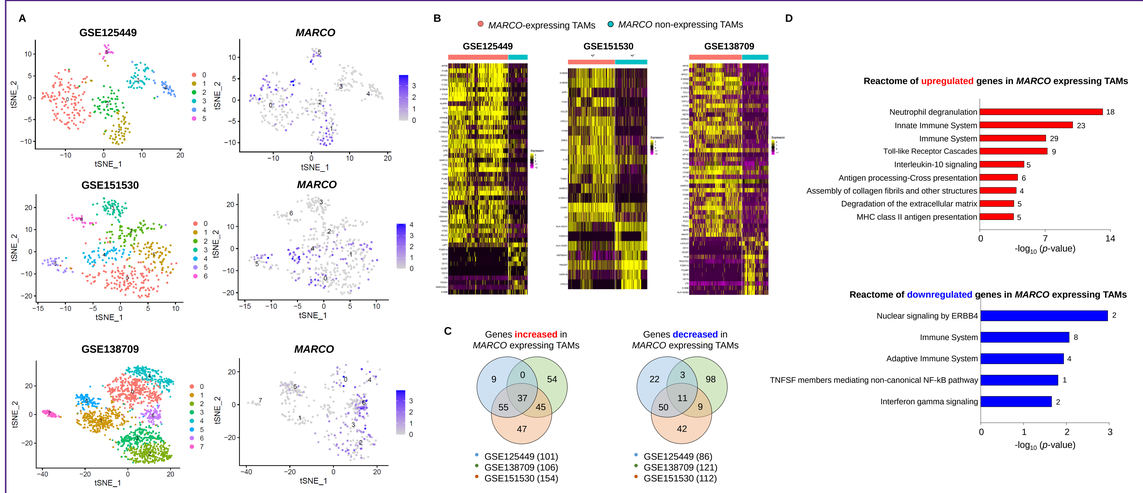

(**A**) Graph-based clustering of TAMs by numbers and analysis of *MARCO* expression therein; (**B**) Heatmaps of differentially expressed genes (|logFC|<1, adjusted p-value < 0.01) between *MARCO* expressing and non-expressing TAMs in human iCCA; (**C**) Volcano plots including genes that are increased or decreased in *MARCO*-expressing tumour infiltrating macrophages in 3 studies; (**D**) Reactome analysis of the commonly upregulated or downregulated genes in *MARCO*-expressing TAMs in comparison to *MARCO* non-expressing TAMs in 3 studies.

Figure 3: Association of *MARCO* to the TME in iCCA

A

Jusakul cohort

Cell type	Spearman (r)	*p*-value	Association with *MARCO*
Macrophages	0.432	6.59E-05	Positively associated
Macrophages (M2)	0.377	0.0006	Positively associated
Dendritic cells	0.343	0.0018	Positively associated
Monocytes	0.327	0.003	Positively associated
Neutrophils	0.302	0.0063	Positively associated
Macrophages (M1)	0.298	0.0071	Positively associated
Fibroblasts	0.296	0.0075	Positively associated
Eosinophils	0.292	0.0085	Positively associated
Plasma cells	0.279	0.0117	Positively associated
B cells	0.260	0.01923	Positively associated
CD4+ T cells	0.254	0.02224	Positively associated
Mast cells	0.232	0.03764	
T cells gamma delta	0.214	0.05473	
CD8+ T cells	0.200	0.07289	
T regulatory cells	0.190	0.08893	
Cytotoxic cells	0.189	0.09181	
Natural Killer cells	0.175	0.1181	
Endothelial cells	0.150	0.1796	

B

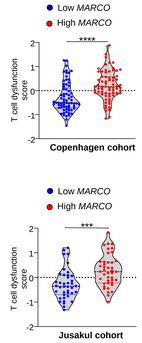

(**A**) Correlation of *MARCO* expression with bioinformatic estimates of cell types using ConsensusTME in human iCCA; (**B**) Association of *MARCO* expression with T cell dysfunctionality in iCCA using the TIDE algorithm.

Figure 4: Role of *Marco* in experimental models of cholangiocarcinogenesis

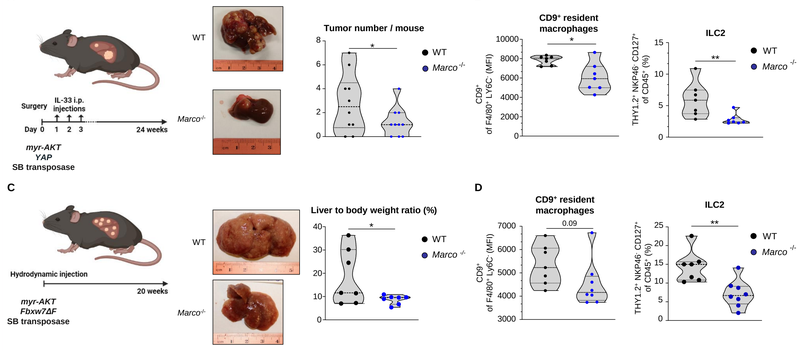

(**A**) Schematic representation of WT and *Marco*$^{-/-}$ mice that were subjected to a biliary tract oncogene transduction of *myr-AKT* and *YAP* combined with a partial bile duct ligature and subsequent systemic IL-33 administration. Mice were sacrificed 24 weeks after surgery and the tumour number per mouse was assessed; (**B**) Mean fluorescence intensity (MFI) of CD9^{+} in liver resident macrophages and percentage of type 2 innate lymphoid cell (ILC2) population of total immune cells (CD45^{+}); (**C**) Schematic representation of a iCCA mouse model based on the hydrodynamic administration of AKT, Fbxw7ΔF and SB transposase. Mice were sacrificed 20 weeks after; (**D**) MFI of CD9+ in liver resident macrophages and percentage of ILC2 population of total immune cells (CD45^{+}).

Figure 5: Role of *Marco* in iCCA progression *in vivo*

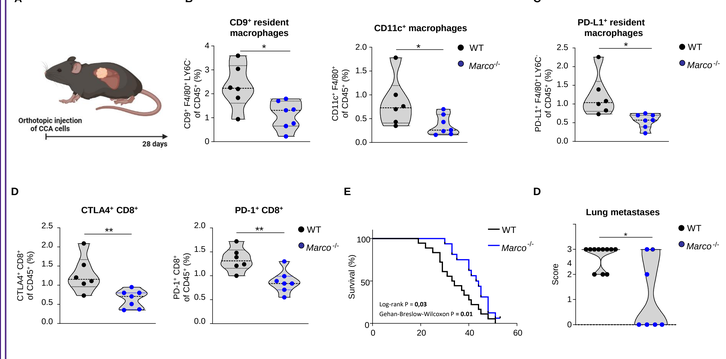

(**A**) Schematic representation of the orthotopic iCCA mouse model carried out in WT and *Marco*$^{-/-}$ mice; (**B**) Percentage of CD9^{+} liver resident macrophages and CD11c^{+} macrophages of total immune cells (CD45^{+}); (**C**) Percentage of PD-L1^{+} liver resident macrophages, (**D**) CTLA-4^{+} and PD-1^{+} cytotoxic T cells of total immune cells (CD45^{+}); (**E**) Survival experiment of the iCCA orthotopic mouse model; (**F**) Score of lung metastasis in WT and *Marco*$^{-/-}$ mice subjected to the orthotopic iCCA mouse model.

CONCLUSIONS

- ***MARCO* expression is lower in iCCA liver tissue in comparison to surrounding non-tumoral liver tissue and normal bile duct regardless the mutational profile. Moreover, high levels of *MARCO* are associated to a worse prognosis in terms of overall survival (OS).**
- ***MARCO* is expressed in a subtype of TAMs associated with an immunosuppressive phenotype in iCCA.**
- ***MARCO* expression levels are strongly associated with the relative abundance of immune cell types involved in tumour progression and with T cell dysfunction in iCCA.**
- ***Marco* deficiency protects mice from tumorigenesis and halts tumoural progression in murine models of iCCA.**